© IWA Publishing 2020
170

Water Practice & Technology Vol 15 No 1
doi: 10.2166/wpt.2020.008

Adsorption behavior of Cr(VI) by N-doped biochar derived from bamboo

Bei Chu[a,*], Kento Terao[b], Yoshimasa Amano[c,d] and Motoi Machida[c,d]

[a] Graduate School of Science and Engineering, Chiba University, Yayoi-cho 1-33, Inage-ku, Chiba 263-8522, Japan

[b] Faculty of Engineering, Chiba University, Yayoi-cho 1-33, Inage-ku, Chiba 263-8522, Japan

[c] Graduate School of Engineering, Chiba University, Yayoi-cho 1-33, Inage-ku, Chiba 263-8522, Japan

[d] Safety and Health Organization, Chiba University, Yayoi-cho 1-33, Inage-ku, Chiba 263-8522, Japan

*Corresponding author. E-mail: chubei@chiba-u.jp

Abstract

In this study, N-doped biochar BZ-9.5AG-30 min was prepared from bamboo by using $ZnCl_2$ as activator and heat treated at 950 °C under NH_3 gas flow for the removal of Cr(VI). The adsorbent was characterized by BET, and the amount of introduced nitrogen content and nitrogen species on BZ-9.5AG-30 min was examined by CHN elemental analyzer and X-ray photoelectron spectroscopy, respectively. Herein, the obtained BZ-9.5AG-30 min had a high specific surface area (1,610 m^2/g) and high N content (4.52%). The pH of the solution had a great influence on the adsorption process, indicating that the acid condition is conducive to the adsorption process of Cr(VI). Adsorption equilibrium data of Cr(VI) were analyzed by the Langmuir and the Freundlich models. The adsorption equilibrium data were well described by the Langmuir model, and BZ-9.5AG-30 min has excellent adsorption capacity for Cr(VI) (4.31 mmol/g). BZ-9.5AG-30 min showed superior recyclability, and after five times regenerations, the adsorption capacity of BZ-9.5AG-30 min still had 63% of the initial adsorption capacity.

Key words: adsorption, bamboo, Cr(VI) removal, N-doped biochar

INTRODUCTION

Heavy metal wastewater pollution triggered by organic dyes has been recognized as a global issue of concern (Farajzadeh & Monji 2004). Cr(VI) is a common toxic heavy metal, which widely exists in manufacturing and dyeing wastewater, electroplating wastewater and other industrial wastewater (Lyu *et al.* 2017; Xiao *et al.* 2018). Cr(VI) has different compounds in aqueous solution, such as $Cr_2O_7^{2-}$, CrO_4^{2-}, and $HCrO_4^-$ (Peng *et al.* 2017), and Cr(VI) has approximately 100 times higher toxicity than Cr(III) (Shen & Wang 1995; Dong *et al.* 2017). Cr(VI) causes harmful effects on the human body due to its strong oxidizing characteristic and can be easily absorbed and accumulated (Naghipour *et al.* 2018), especially by the kidneys, stomach, and liver (Miretzky & Cirelli 2010). WHO has set the Cr(VI) lower limit of drinking water to be 0.05 mg/L or less (Bansal *et al.* 2009). Therefore, it is necessary to carry out effluent treatment before discharging Cr(VI) wastewater into the environment.

At present, conventional treatment methods for Cr(VI)-containing wastewater include reduction (Pinos *et al.* 2016), ion exchange (Rapti *et al.* 2016), biological treatment method (Zeng *et al.* 2019), and adsorption (Ramavandi *et al.* 2014). Among these, adsorption is a better method because of its high efficiency, low cost and simplicity of design (Yan *et al.* 2017; Jaafari & Yaghmaeian 2019). Carbon adsorbents generally include activated carbon, carbon molecular sieves and carbon-containing nanomaterials (Mohan *et al.* 2005). Activated carbon is the most widely used carbon adsorption

Water Practice & Technology Vol 15 No 1
doi: 10.2166/wpt.2020.008

material (Lalvani *et al.* 1998). Activated carbon is mostly made from bamboo, wood and other raw materials, which are activated after carbonization at high temperature (Salas-Enríquez *et al.* 2019). Generally, activated carbon can be divided into granular activated carbon and powdered activated carbon according to particle size. Activated carbon has a high specific surface area of up to 1,500 m^2/g, and there are many kinds of oxygen-containing functional groups on the surface.

Biochar is an activated carbon like adsorbent (Tan *et al.* 2016). However, due to the lack of porous structure, the specific surface area of most biochar is relatively low. To overcome this shortcoming, the primary activator used is $ZnCl_2$, H_3PO_4, KOH, and NaOH. Among them, $ZnCl_2$ activation method is relatively sophisticated method (Su *et al.* 2015). Recent studies have reported that nitrogen (N) doping can enhance the adsorption capacity of activated carbon for anions such as nitrate (Goto *et al.* 2017). Since the presence of quaternary nitrogen on the surface of nitrogen-doped activated carbon, it acts as a positively charged adsorption site on carbon, surface which is beneficial to the adsorption of various anions (Yoo *et al.* 2018).

Bamboo could be regarded as cheaply available biochar material (Su & Dong 2019). A large number of low-value bamboo wastes will be produced in the process of bamboo exploitation, processing, and utilization. The effective utilization rate of bamboo wastes is only about 35–40%. Bamboo waste, if discarded, decayed, buried or burned, not only will cause environmental pollution, but also a waste of bamboo resources. Bamboo contains a lot of cellulose and lignin, and its resource utilization is extensive. Biochar materials can be prepared by treating bamboo forest solid wastes, which have good adsorption effect on heavy metals and organic pollutants in water.

Based on these considerations, in this work, the commercial bamboo chips were further activated by $ZnCl_2$ and heat treated at 950 °C under NH_3 gas flow, in order to increase the adsorption capacity for Cr(VI) in aqueous solution.

MATERIALS AND METHODS

Materials

The feedstock for the production of biochar was willow residues pruned from moso bamboo. Moso bamboo obtained in Aichi prefecture, Japan, was cut into chips and used as a precursor for preparation of adsorbent.

The bamboo chips were dried in an oven at 110 °C for 1 h. In this study, using the $ZnCl_2$ as an activator, the prepared bamboo chips were impregnated with $ZnCl_2$ solution at a ratio of 3 g-$ZnCl_2$/g-bamboo, and then the mixture was dried in an oven at 110 °C overnight. The resulting mixture was pyrolyzed for 1 h at 400 °C under N_2 atmosphere in a tubular furnace. The prepared biochar was placed in 1 M HCl solution and stirred for 1 h, rinsed in a Soxhlet extractor for 24 h, and dried at 110 °C overnight. The obtained samples were referred to as BZ.

N-doped biochar were prepared from BZ. The prepared BZ was heated from room temperature to 600 °C under a helium atmosphere in a tubular furnace, then the helium gas was directly replaced by NH_3 gas, then heated up to 950 °C and kept there for 0, 15, 30 and 45 minutes. Finally, the NH_3 gas was changed to helium and the samples were cooled to room temperature. The obtained samples were referred to as BZ-9.5AG-*x*min, where *x* is the heating retention time.

Biochar characterization

The specific surface area (S_{BET}), mesopore volume (V_{meso}) and micropore volume (V_{micro}) of the prepared biochar were calculated based on N_2 adsorption/desorption isotherms at −196 °C using a Bellsorp-mini II (MicrotracBEL, Co., Ltd., Japan) surface area analyzer. The elemental composition

Water Practice & Technology Vol 15 No 1
doi: 10.2166/wpt.2020.008

of C, H and N of the adsorbents was determined with a Perkin Elmer 2400 II (Perkin Elmer Japan, Co., Ltd., Japan), and O content was obtained by difference. X-ray photoelectron spectroscopy (XPS) analysis was performed using a JEOL JPS-9030 spectrometer. The concentrations of Cr(VI) solution after batch experiments were determined with an atomic adsorption spectrometer novAA300 (Analytik Jena AG, Germany).

Batch adsorption

The removal of Cr(VI) by the biochar was examined by measuring the concentrations of Cr(VI) in a batch system. All batch experiments were carried out in Erlenmeyer flasks. Batch experiments were conducted in 30 mL Erlenmeyer flasks, with 0.02 g of the sample put into a flask containing 20 mL of Cr(VI) solution with various initial concentrations. The flasks were agitated in a water bath shaker at 25 °C at the speed of 100 rpm. The adsorbed amount of Cr(VI) per unit mass of adsorbent was calculated by Equation (1):

$$Q_e = (C_0 - C_e) \times V/m \tag{1}$$

where m (g) is the mass of the biochar, V (L) is the volume of the Cr(VI) solution, C_0 (mmol/L) represents the initial concentration of Cr(VI), C_e (mmol/L) is the adsorption equilibrium concentration of Cr(VI).

The effect of solution pH on Cr(VI) adsorption was examined by mixing 20 mg of adsorbent with 20 mL of 9 mmol/L Cr(VI) solution. The mixed solution had different pH values, ranging from 2 to 9. The initial pH of Cr(VI) solution was adjusted by 0.1 M HCl and 0.1 M NaOH.

The theoretical equilibrium adsorption capacity of activated carbon for heavy metal ions is an important index to measure its adsorption capacity. Under isothermal conditions, the adsorption phenomena on the adsorbent surface in solution, and the relationship between the amount of adsorption on the adsorbent surface and the equilibrium concentration of the solution, were characterized. The commonly used fitting models are the Langmuir isotherm model and the Freundlich isotherm model. The Langmuir isotherm model is a theoretical formula, which is based on three assumptions: (1) the adsorbent surface is uniform, and the adsorption energy is the same everywhere; (2) the adsorption is a monolayer, and when the adsorbent surface is saturated with the adsorbate, its adsorption capacity reaches the maximum; (3) there is no interaction between the adsorbed molecules (Wu *et al.* 2010). The equation is as follows:

$$\frac{C_e}{Q_e} = \frac{1}{X_m K_L} + \frac{1}{X_m} C_e \tag{2}$$

where, X_m (mmol/g) represents the theoretical maximum adsorbed amount of Cr(VI), and K_L (L/mmol) is the Langmuir constant related to adsorption energy.

The Freundlich isotherm model is an empirical formula, which shows that the adsorption occurs on heterogeneous surfaces and is multiphase adsorption (Luo *et al.* 2018). The expression is as follows:

$$\ln Q_e = \ln K_F + \frac{1}{n} \ln C_e \tag{3}$$

where K_F is the Freundlich constant and $1/n$ is the heterogeneity factor. The greater the value of n, the better the adsorption performance.

The adsorption kinetics of Cr(VI) on biochar samples were studied by mixing 0.2 g of adsorbent with 200 ml of 9 mmol/L Cr(VI) solution, and the concentration was analyzed at disparate time intervals (1, 2, 3, 4, 5, 10, 15, 20, 25, 30, 60, 120, 180, 240, 300, 480, 1,500, and 1,920 min). The data were

Water Practice & Technology Vol 15 No 1
doi: 10.2166/wpt.2020.008

analyzed using both the pseudo-first-order and the pseudo-second-order models. The linearized forms of the models are shown as follows:

$$\ln (Q_e - Q_t) = lnQ_e - k_1 t \tag{4}$$

$$\frac{t}{Q_t} = \frac{1}{k_2 Q_e^2} + \frac{t}{Q_e} \tag{5}$$

where Q_e is the amount of Cr(VI) adsorbed at equilibrium (mmol/g), Q_t is the adsorbed amount of Cr(VI) (mmol/g) at time t (min). k_1 and k_2 are the rate constant of the pseudo-first-order model (L/min) and the pseudo-second-order model (g/mmol•min).

In order to test the regeneration capacity of the biochar, 300 mg of adsorbent was added to an Erlenmeyer flask containing 300 mL of Cr(VI) solution with an initial pH of 2 and an initial concentration of 9 mmol/L. The flasks were shaken at 100 rpm at 25 °C for 24 h to reach apparent equilibrium. Then the mixture was filtered with 0.45 μm filter paper, in the desorption agent, the filtered biochar was washed with distilled water and placed in 300 mL of 1 mol/L NaOH solution at 90 °C for 2 h. The regeneration experiment was repeated in successive adsorption-desorption cycles that were conducted five times.

RESULTS AND DISCUSSION

Characterization of biochar

The elemental composition of oxidized biochar with different NH_3 retention times is shown in Table 1. It can be seen from Table 1 that the N content of BZ was only 0.4%; by contrast, the N content of biochar after NH_3 treatment increased. As the NH_3 retention time increased from 0 min to 30 min, the N content increased from 3.06% to 4.52%. And as the NH_3 retention time increased to 45 min, the N content of biochar decreased to 2.83%. This shows that the N content of biochar reached its maximum when the NH_3 retention time was 30 min. Therefore, BZ-9.5AG-30 min is expected to have higher removal efficiency of Cr(VI).

Table 1 | Elemental composition of BZ-9.5AG-30 min

Adsorbent	C [wt%]	H [wt%]	N [wt%]	O[a] [wt%]
BZ	90.37	1.41	0.20	7.92
BZ-9.5AG-0 min	91.29	0.49	3.06	5.16
BZ-9.5AG-15 min	90.70	0.44	3.50	5.36
BZ-9.5AG-30 min	88.66	0.39	4.52	6.43
BZ-9.5AG-45 min	90.58	0.41	2.83	6.18

[a]Calculated by difference.

The nitrogen adsorption-desorption isotherm curve of the BZ-9.5AG-*x*min is shown in Figure 1. From Figure 1, a type I isotherm was observed, which indicates the existence of a mainly microporous structure. The specific surface area (BET) and micro-/mesoporous structure parameters of the adsorbent were calculated and are shown in Table 2. It can be seen that the specific surface area (S_{BET}) of biochar decreased after the beginning of NH_3 gas introduction, but the specific surface area of biochar increased with the increased NH_3 retention time. This may be due to the formation of N-containing functional groups on the surface of the biochar at the beginning of NH_3 introduction, thus reducing

Water Practice & Technology Vol 15 No 1
doi: 10.2166/wpt.2020.008

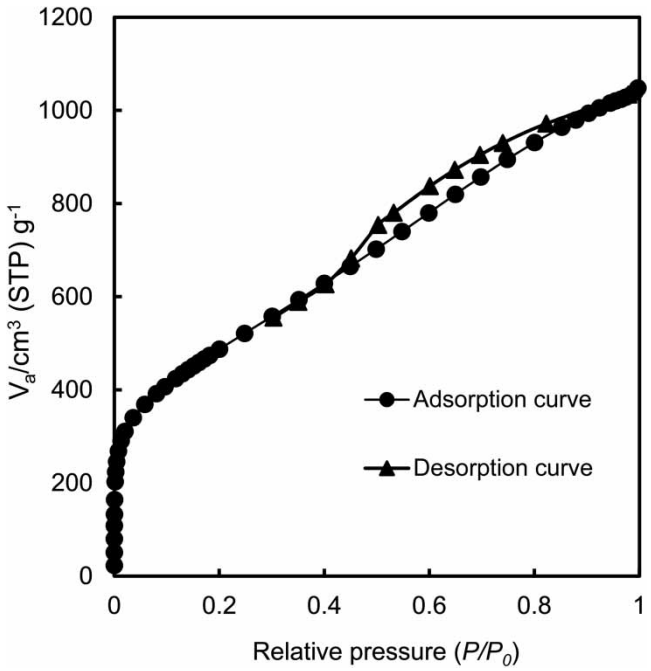

Figure 1 | Nitrogen adsorption isotherm of BZ-9.5AG-30 min.

Table 2 | Textural and surface properties of each prepared biochar

Adsorbent	S_{BET} [m^2/g]	V_{total} [cm^3/g]	V_{micro} [cm^3/g]	V_{meso} [cm^3/g]
BZ	1,399	0.75	0.74	0.01
BZ-9.5AG-0 min	1,122	0.55	0.55	0.01
BZ-9.5AG-15 min	1,277	0.63	0.63	0.01
BZ-9.5AG-30 min	1,610	0.85	0.85	0.01
BZ-9.5AG-45 min	1,869	1.00	0.99	0.01

the surface area. With the increased NH_3 retention time at high temperature, the microporous structure was developed continuously and the specific surface area of the biochar increased.

Adsorption isotherms and adsorption capacity

Adsorption isotherms of Cr(VI) for the BZ and BZ-9.5AG-30 min are shown in Figure 2. Both Langmuir and Freundlich models were used to fit the adsorption data. The adsorption process of Cr(VI) at 25 °C and the different isotherm constants determined are presented in Table 3. The R^2 values of the Langmuir model were larger than those of the Freundlich model, indicating that the Langmuir models can be a good description of Cr(VI) adsorption behavior. The Langmuir isotherm is usually used to describe monolayer adsorption on a homogenous surface, indicating that Cr(VI) adsorption onto BZ and BZ-9.5AG-30 min tended to be monolayer adsorption. BZ and BZ-9.5AG-30 min all exhibited high adsorption capacity for Cr(VI). Comparatively, the maximum adsorbed amount (X_m) of Cr(VI) onto BZ-9.5AG-30 min was larger than the X_m of BZ, which indicated that N-doping biochar has better adsorption capacity for Cr(VI). The increase in the adsorbed amount can be explained by the increase of specific surface area and nitrogen content. Compared with BZ, BZ-9.5AG-30 min had a larger specific surface area and total pore volume, so it can provide more adsorption sites.

Water Practice & Technology Vol 15 No 1
doi: 10.2166/wpt.2020.008

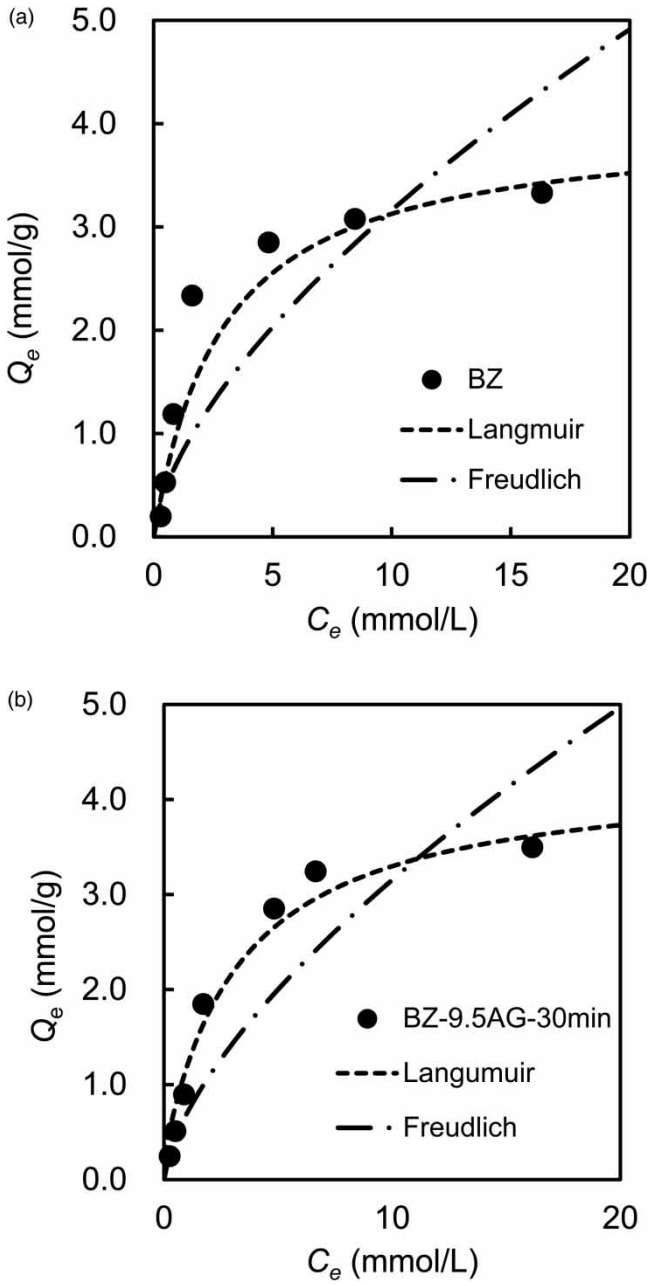

Figure 2 | Adsorption isotherms of BZ (a) and BZ-9.5AG-30 min (b) for Cr(VI).

Table 3 | Langmuir and Freundlich adsorption isotherm parameters of Cr(VI) at 298 K in aqueous solutions

	Langmuir model			Freudlich model		
	X_m (mmol/g)	K_L (L/mmol)	R^2	1/*n*	K_F	R^2
BZ	3.81	0.38	0.95	0.64	0.73	0.80
BZ-9.5AG-30 min	4.31	0.32	0.98	0.66	0.69	0.92

With the increase of nitrogen content, more quaternary nitrogen (N-Q) can be formed on the surface of the biochar. Positive charges on quaternary nitrogen can provide more adsorption sites for anions, thus increasing the adsorption of Cr(VI) (Yoo *et al.* 2018).

Water Practice & Technology Vol 15 No 1
doi: 10.2166/wpt.2020.008

Comparison with values in the literature (Table 4) shows that BZ-9.5AG-30 min is among the highest carbon adsorbents for Cr(VI) (Karthikeyan *et al.* 2005; Rangabhashiyam & Selvaraju 2015; Zhu *et al.* 2016; Chu *et al.* 2018; Yu *et al.* 2018; Zhang *et al.* 2018), so it has great potential in practical water treatment applications.

Table 4 | Comparison with other similar adsorbents for Cr(VI) removal

Adsorbent	Q_e (mmol/g)	Reference
Swietenia mahagoni shell	1.13	Rangabhashiyam & Selvaraju (2015)
Hevea brasilinesis sawdust AC	0.85	Karthikeyan *et al.* (2005)
Biochar derived from waste water hyacinth	0.46	Yu *et al.* (2018)
Bismuth modified biochar	0.23	Zhu *et al.* (2016)
Biochar derived from *Melia azedarach* wood	0.49	Zhang *et al.* (2018)
Ion exchange resin HP555	3.69	Chu *et al.* (2018)
N-doped biochar BZ-9.5AG-30 min	4.31	This work

Effect of pH

The initial pH of the solution usually has a great influence on the adsorption capacity of biochar. The effect of initial pH on the adsorption of Cr(VI) by BZ-9.5AG-30 min is shown in Figure 3. For adsorption of Cr(VI), the adsorbed amount of Cr(VI) on BZ-9.5AG-30 min decreased as pH increased from 2 to 9. The effect of initial pH on adsorption can be explained by the surface charge of biochar and the ionic forms of Cr(VI). Cr(VI) exists primarily as an oxyanion, and it exists in different ionic forms in aqueous solution. When solution pH is greater than 6, it presents as CrO_4^{2-}; when pH is ranging between 1.0 and 6.0, it exists as $Cr_2O_7^{2-}$ and $HCrO_4^-$. Therefore, when the solution pH has changed the form of the Cr(VI) ions it will influence the Cr(VI) uptake capacity of the biochar. Moreover, amino groups exist on the surface of N-doped biochar. Under acidic conditions, amino groups present

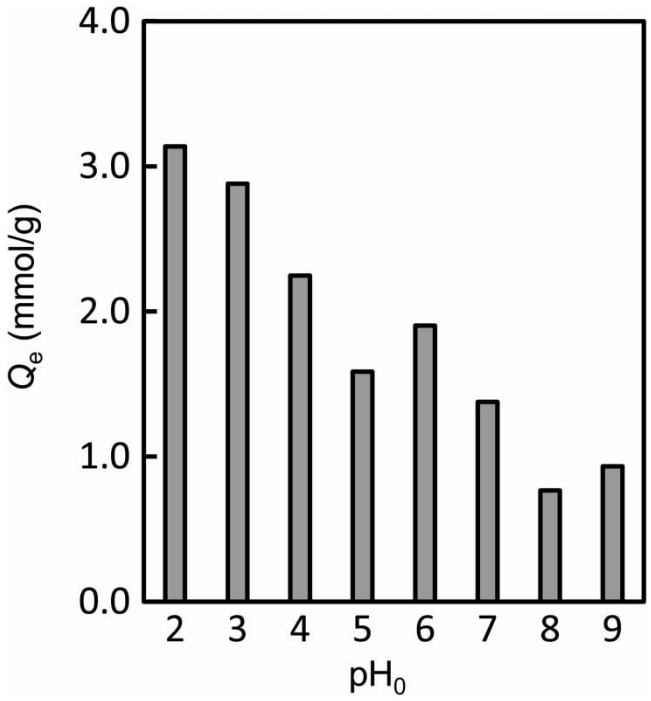

Figure 3 | Effect of initial pH value on Cr(VI) removal.

Water Practice & Technology Vol 15 No 1
doi: 10.2166/wpt.2020.008

as NH_3^+, with positive sites, which are also beneficial to the adsorption of Cr(VI) (Zhao *et al.* 2011). With the increase of pH, the amount of OH^- ions in the solution increases, and the competition between OH^- ions and Cr(VI) ions results in a decrease of the adsorption capacity of biochar to Cr(VI) (Liu *et al.* 2017).

Effect of contact time and adsorption kinetics

The effects of contact time on the adsorption capacity of BZ-9.5AG-30 min for Cr(VI) were also investigated. As shown in Figure 4, is the determination of the relationship between the amount of adsorption of Cr(VI) and time in the range of 0–2,000 min. The adsorption rate of Cr(VI) was initially higher, reaching 86% of the maximum adsorption capacity at 480 minutes, and the adsorption capacity (Q_t) would not change after 1,000 minutes. So the optimum adsorption time of BZ-9.5AG-30 min for Cr(VI) was about 1,000 min. The experimental data in Figure 4 were fitted with the pseudo-first-order model and pseudo-second-order model, and the results of the kinetic analysis are shown in Table 5. As shown in Table 5, the R^2 values of the pseudo-first-order model and the pseudo-second-order model are both higher than 0.95; however, the R^2 value of the pseudo-second-order model was larger than that of the pseudo-first-order model and larger than 0.99, which indicates that the pseudo-second-order model can better describe the adsorption of BZ on Cr(VI). These facts suggest that the adsorption behavior is mainly governed by diffusion control mechanism in Cr(VI) solution.

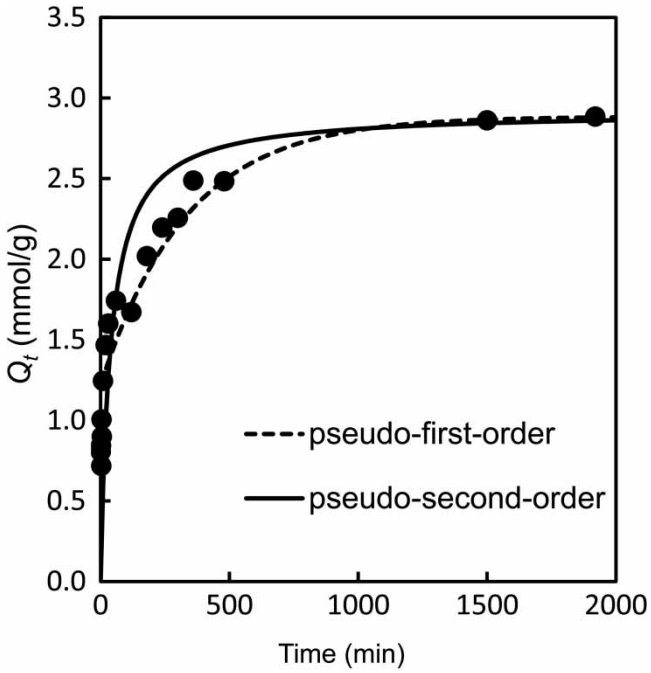

Figure 4 | Cr(VI) adsorption kinetic by BZ-9.5AG-30 min.

Table 5 | Kinetic parameters for Cr(VI) adsorption onto BZ-9.5AG-30 min

Pseudo-first order			Pseudo-second order		
Q_e (mmol/g)	k_1 (min^{-1})	R^2	Q_e (mmol/g)	k_2 (g/mmol min)	R^2
2.89	0.003	0.97	2.92	0.008	0.998

Water Practice & Technology Vol 15 No 1
doi: 10.2166/wpt.2020.008

XPS analysis

The XPS spectra measurement was performed to investigate the surface chemical state and elemental changes of BZ-9.5AG-30 min before and after adsorption. As shown in Figure 5(a), before the adsorption of Cr (VI), the XPS spectra of biochar showed three peaks, C 1s (284 eV), N 1s (400 eV) and O 1s (531 eV), respectively. After the experiment of Cr(VI) adsorption, a very obvious peak appeared at 578 eV, which is assigned to the Cr $2p_{3/2}$ energy level, suggesting that Cr(VI) was successfully adsorbed on the biochar. The N1s spectra of BZ-9.5AG-30 min before and after the removal of Cr(VI) are shown in Figure 5(b) and 5(c). The N 1s spectrum was resolved into four individual

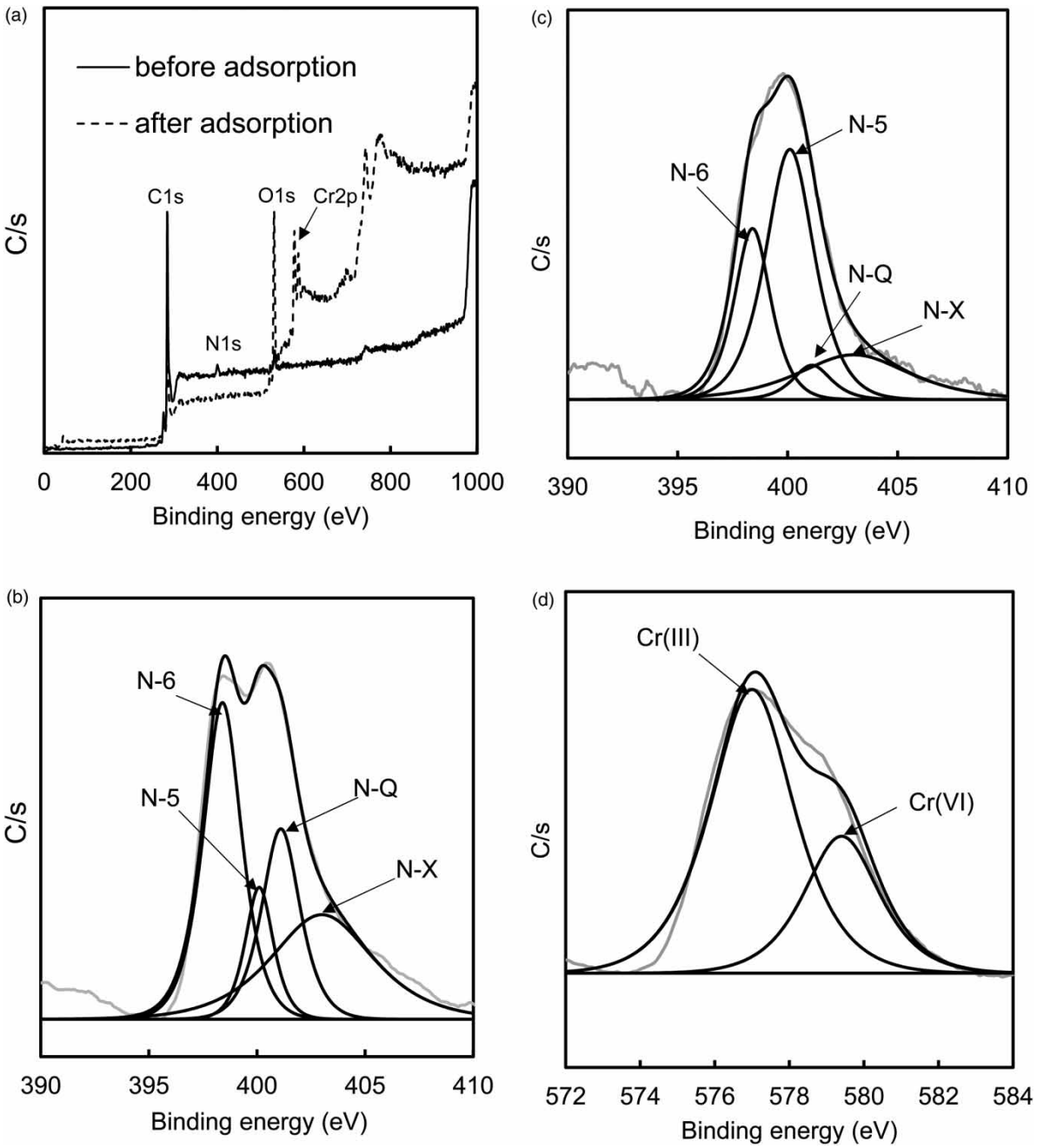

Figure 5 | (a) XPS survey spectra of BZ-9.5AG-30 min before and after Cr(VI) adsorption; (b) N 1 s spectrum of BZ-9.5AG-30 min before Cr(VI) adsorption; (c) N 1 s spectrum of BZ-9.5AG-30 min after Cr(VI) adsorption; (d) Cr 2p spectrum of BZ-9.5AG-30 min after Cr(VI) adsorption.

Water Practice & Technology Vol 15 No 1
doi: 10.2166/wpt.2020.008

peaks at 398.7 eV, 400.4 eV, 401.3 eV and 403.3 eV, which are assigned to pyridinic nitrogen (N-6), pyrrolic nitrogen (N-5), quaternary nitrogen (N-Q) and pyridine-N-oxide (N-X), respectively. Among them, because N-Q has a positive charge, the adsorption capacity of anions should be increased. Notably, as shown in Table 6, the percentage of N-Q in BZ-9.5AG-30 min decreases from 22.3% to 5.5% after adsorption, and this would be because the reduction process of Cr(VI) consumes the positive charge on the adsorbent surface, resulting in the decrease of N-Q.

Table 6 | Relative surface atomic ratios of different N species in BZ-9.5AG-30 min before and after Cr(VI) adsorption

	N-6 (%)	N-5 (%)	N-Q (%)	N-X (%)
Before adsorption	37.1	11.4	22.3	29.2
After adsorption	25.9	50.4	5.5	18.2

Figure 5(d) shows the Cr $2p_{3/2}$ spectrum, and the Cr $2p_{3/2}$ spectrum is divided into two peaks at 577.6 eV and 579.5 eV, which were assigned to Cr(III) and Cr(VI). The adsorbed chromium predominantly existed in Cr(III), and only a small amount was present as Cr(VI). As shown in Figure 5(d), 69.7% of the adsorbed chromium existed in trivalent form, and the remaining 30.3% was present as Cr(VI).

Regeneration experiment

In order to evaluate the recoverability of N-doped biochar BZ, five cycles of adsorption-desorption experiments were carried out on N-doped biochar BZ-9.5AG-30 min. Figure 6 shows the adsorption capacity of BZ-9.5AG-30 min for Cr(VI) in the function of the adsorption-desorption cycles. After five time regenerations, the adsorption capacity of BZ-9.5AG-30 min still had 63% of the initial adsorption capacity, so it had better regeneration ability than our previous study (Chu *et al.* 2018).

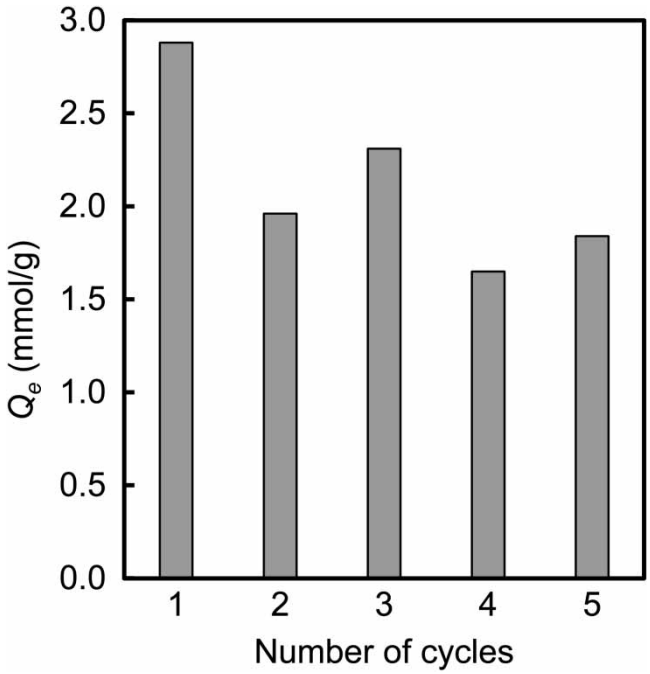

Figure 6 | The regeneration adsorptive performance of BZ-9.5AG-30 min after five cycles.

Water Practice & Technology Vol 15 No 1
doi: 10.2166/wpt.2020.008

CONCLUSIONS

In conclusion, we have successfully prepared N-doped biochar adsorbent BZ-9.5AG-30 min for heavy metal Cr(VI) removal. The Cr(VI) removal experiments showed that BZ-9.5AG-30 min had a high adsorption capacity (4.31 mmol/g) of Cr(VI), which was much higher than previous reports. The effect of pH has shown that the highest adsorption capacity of Cr(VI) by BZ-9.5AG-30 min was at pH 2. The adsorption reaction conformed to the Langmuir model, and the kinetic analyses indicated that the adsorption of Cr(VI) by BZ-9.5AG-30 min fitted well with the pseudo-second-order model. After five regeneration experiments, BZ-9.5AG-30 min showed superior recyclability, and therefore, BZ-9.5AG-30 min is expected to be a promising adsorbent for the efficient removal of Cr(VI) from wastewater.

ACKNOWLEDGEMENTS

Gratitude is greatly extended to Prof. Dr. Fumio Imazeki, the head of Safety and Health Organization, Chiba University, for his financial support on our study. The first author also acknowledges the kind support of the Japanese Government (MEXT) for the scholarship.

REFERENCES

Bansal, M., Singh, D. & Garg, V. 2009 A comparative study for the removal of hexavalent chromium from aqueous solution by agriculture wastes' carbons. *Journal of Hazardous Materials* **171**(1–3), 83–92.

Chu, B., Yamoto, M., Amano, Y. & Machida, M. 2018 Adsorption, reduction and regeneration behavior of high surface area activated carbon in removal of Cr (VI). *Desalination and Water Treatment* **136**, 395–404.

Dong, H., Deng, J., Xie, Y., Zhang, C., Jiang, Z., Cheng, Y., Hou, K. & Zeng, G. 2017 Stabilization of nanoscale zero-valent iron (nZVI) with modified biochar for Cr (VI) removal from aqueous solution. *Journal of Hazardous Materials* **332**, 79–86.

Farajzadeh, M. A. & Monji, A. B. 2004 Adsorption characteristics of wheat bran towards heavy metal cations. *Separation and Purification Technology* **38**(3), 197–207.

Goto, T., Amano, Y. & Machida, M. 2017 Preparation of anion exchangers derived from melamine sponge and its adsorption characteristics of nitrate ion. *Journal of Chemical Engineering of Japan* **50**(9), 692–695.

Jaafari, J. & Yaghmaeian, K. 2019 Optimization of heavy metal biosorption onto freshwater algae (Chlorella coloniales) using response surface methodology (RSM). *Chemosphere* **217**, 447–455.

Karthikeyan, T., Rajgopal, S. & Miranda, L. R. 2005 Chromium (VI) adsorption from aqueous solution by Hevea Brasilinesis sawdust activated carbon. *Journal of Hazardous Materials* **124**(1–3), 192–199.

Lalvani, S., Wiltowski, T., Hübner, A., Weston, A. & Mandich, N. 1998 Removal of hexavalent chromium and metal cations by a selective and novel carbon adsorbent. *Carbon* **36**(7–8), 1219–1226.

Liu, C., Jin, R.-N., Ouyang, X.-k. & Wang, Y.-G. 2017 Adsorption behavior of carboxylated cellulose nanocrystal – polyethyleneimine composite for removal of Cr (VI) ions. *Applied Surface Science* **408**, 77–87.

Luo, H., Huang, X., Luo, Y., Li, Z., Li, L., Gao, C., Xiong, J. & Li, W. 2018 Adsorption behavior and mechanism of acidic blue 25 dye onto cucurbit [8] uril: a spectral and DFT study. *Spectrochimica Acta Part A: Molecular and Biomolecular Spectroscopy* **193**, 125–132.

Lyu, H., Tang, J., Huang, Y., Gai, L., Zeng, E. Y., Liber, K. & Gong, Y. 2017 Removal of hexavalent chromium from aqueous solutions by a novel biochar supported nanoscale iron sulfide composite. *Chemical Engineering Journal* **322**, 516–524.

Miretzky, P. & Cirelli, A. F. 2010 Cr (VI) and Cr (III) removal from aqueous solution by raw and modified lignocellulosic materials: a review. *Journal of Hazardous Materials* **180**(1–3), 1–19.

Mohan, D., Singh, K. P. & Singh, V. K. 2005 Removal of hexavalent chromium from aqueous solution using low-cost activated carbons derived from agricultural waste materials and activated carbon fabric cloth. *Industrial & Engineering Chemistry Research* **44**(4), 1027–1042.

Naghipour, D., Taghavi, K., Ashournia, M., Jaafari, J. & Arjmand Movarrekh, R. 2018 A study of Cr (VI) and NH4+ adsorption using greensand (glauconite) as a low-cost adsorbent from aqueous solutions. *Water and Environment Journal* **34** (1), 45–56.

Peng, Z., Xiong, C., Wang, W., Tan, F., Xu, Y., Wang, X. & Qiao, X. 2017 Facile modification of nanoscale zero-valent iron with high stability for Cr (VI) remediation. *Science of The Total Environment* **596**, 266–273.

Pinos, V., Dafinov, A., Medina, F. & Sueiras, J. 2016 Chromium (VI) reduction in aqueous medium by means of catalytic membrane reactors. *Journal of Environmental Chemical Engineering* **4**(2), 1880–1889.

Water Practice & Technology Vol 15 No 1
doi: 10.2166/wpt.2020.008

Ramavandi, B., Asgari, G., Faradmal, J., Sahebi, S. & Roshani, B. 2014 Abatement of Cr (VI) from wastewater using a new adsorbent, cantaloupe peel: taguchi L 16 orthogonal array optimization. *Korean Journal of Chemical Engineering* **31**(12), 2207–2214.

Rangabhashiyam, S. & Selvaraju, N. 2015 Efficacy of unmodified and chemically modified Swietenia mahagoni shells for the removal of hexavalent chromium from simulated wastewater. *Journal of Molecular Liquids* **209**, 487–497.

Rapti, S., Pournara, A., Sarma, D., Papadas, I. T., Armatas, G. S., Tsipis, A. C., Lazarides, T., Kanatzidis, M. G. & Manos, M. J. 2016 Selective capture of hexavalent chromium from an anion-exchange column of metal organic resin–alginic acid composite. *Chemical Science* **7**(3), 2427–2436.

Salas-Enríquez, B. G., Torres-Huerta, A. M., Conde-Barajas, E., Domínguez-Crespo, M. A., Negrete-Rodríguez, M. L., Dorantes-Rosales, H. J. & López-Oyama, A. B. 2019 Stabilized landfill leachate treatment using Guadua amplexifolia bamboo as a source of activated carbon: kinetics study. *Environmental Technology* **40**(6), 768–783.

Shen, H. & Wang, Y.-T. 1995 Simultaneous chromium reduction and phenol degradation in a coculture of Escherichia coli ATCC 33456 and Pseudomonas putida DMP-1. *Applied and Environmental Microbiology* **61**(7), 2754–2758.

Su, R. & Dong, X. 2019 Preparation and electrochemical properties of bamboo-based carbon for lithium-ion-battery anode material. *International Journal of Electerochemical Science* **14**(3), 2452–2461.

Su, Y., Sun, X., Zhou, X., Dai, C. & Zhang, Y. 2015 Zero-valent iron doped carbons readily developed from sewage sludge for lead removal from aqueous solution. *Journal of Environmental Sciences* **36**, 1–8.

Tan, X.-f., Liu, Y.-g., Gu, Y.-l., Xu, Y., Zeng, G.-m., Hu, X.-j., Liu, S.-b., Wang, X., Liu, S.-m. & Li, J. 2016 Biochar-based nano-composites for the decontamination of wastewater: a review. *Bioresource Technology* **212**, 318–333.

Wu, F.-C., Tseng, R.-L. & Juang, R.-S. 2010 A review and experimental verification of using chitosan and its derivatives as adsorbents for selected heavy metals. *Journal of Environmental Management* **91**(4), 798–806.

Xiao, R., Wang, J. J., Li, R., Park, J., Meng, Y., Zhou, B., Pensky, S. & Zhang, Z. 2018 Enhanced sorption of hexavalent chromium [Cr (VI)] from aqueous solutions by diluted sulfuric acid-assisted MgO-coated biochar composite. *Chemosphere* **208**, 408–416.

Yan, Y., An, Q., Xiao, Z., Zheng, W. & Zhai, S. 2017 Flexible core-shell/bead-like alginate@ PEI with exceptional adsorption capacity, recycling performance toward batch and column sorption of Cr (VI). *Chemical Engineering Journal* **313**, 475–486.

Yoo, P., Amano, Y. & Machida, M. 2018 Adsorption of nitrate onto nitrogen-doped activated carbon fibers prepared by chemical vapor deposition. *Korean Journal of Chemical Engineering* **35**(12), 2468–2473.

Yu, J., Jiang, C., Guan, Q., Ning, P., Gu, J., Chen, Q., Zhang, J. & Miao, R. 2018 Enhanced removal of Cr (VI) from aqueous solution by supported ZnO nanoparticles on biochar derived from waste water hyacinth. *Chemosphere* **195**, 632–640.

Zeng, Q., Hu, Y., Yang, Y., Hu, L., Zhong, H. & He, Z. 2019 Cell envelop is the key site for Cr (VI) reduction by Oceanobacillus oncorhynchi W4, a newly isolated Cr (VI) reducing bacterium. *Journal of Hazardous Materials* **368**, 149–155.

Zhang, X., Lv, L., Qin, Y., Xu, M., Jia, X. & Chen, Z. 2018 Removal of aqueous Cr (VI) by a magnetic biochar derived from Melia azedarach wood. *Bioresource Technology* **256**, 1–10.

Zhao, G., Li, J., Ren, X., Chen, C. & Wang, X. 2011 Few-layered graphene oxide nanosheets as superior sorbents for heavy metal ion pollution management. *Environmental Science & Technology* **45**(24), 10454–10462.

Zhu, N., Yan, T., Qiao, J. & Cao, H. 2016 Adsorption of arsenic, phosphorus and chromium by bismuth impregnated biochar: adsorption mechanism and depleted adsorbent utilization. *Chemosphere* **164**, 32–40.